*Annals of Science and Technology* - A, Vol 8 (2): 63-73, 2023
Copyright: An Official *Journal* of the Nigerian Young Academy
ISSN: 2 544 6320

sciendo

**ARTICLE**

# Investigating the Impacts of Tropospheric Parameters on Received Signal Strength of the Mobile Communication System

**Bukola H. Akinwole [1*], Abayomi I.O. Yussuff [2]**

*[1] Department of Electrical/Electronic Engineering, University of Port Harcourt, Rivers State*
*[2]Department of Electronic & Computer Engineering, Lagos State University, Nigeria*

***Received 26th September, 2022, Accepted 24th September, 2023***
**DOI: 10.2478/ast-2023-0016**

**Corresponding author*
*Bukola H. Akinwole, Email bakinwol @gmail.com; Tel: +234 8037086238*

**Abstract**

Radio communication systems are crucial for information transmission, but they face challenges like interference and fading, which significantly impact network efficiency. Understanding propagation-related issues is crucial for optimizing networks. This study examined the influence of tropospheric parameters on the Received Signal Strength (RSS) of the Globacom communication system in Rivers State. Four tropospheric variables (air temperature, relative humidity, atmospheric pressure, and wind speed) are collected from the River State University of Science and Technology (RSUST) Environmental and Climatic Observatory Program. The results of the correlation analysis indicated a direct linear correlation between air temperature and RSS. In contrast, wind speed displayed an indirect relationship, while the remaining parameters demonstrated an inverse linear relationship. Multiple linear regression (MLR) and multiple linear perceptron (MLP) models were developed to accurately predict the impacts of tropospheric parameters on RSS. A supervised-learning three-layered MLP feed-forward neural network was employed, consisting of 10 distinct MLP NN models. The Levenberg-Marquardt (LM) learning algorithm was used in training and validating the MLP NN models. The MLP 4-40-1 model showed an exceptional understanding of the non-linear relationship between the tropospheric parameters and RSS. The MLR model exhibited a weaker correlation coefficient of 0.2164, while the MLP demonstrated a stronger correlation coefficient of 0.7942. Additionally, the MLP 4-40-1 model outperformed the MLR model in terms of Root Mean Square Error (RMSE) and Mean Absolute Percentage Error (MAPE), achieving an accuracy of 0.2480 RMSE and 12.9963% MAPE, while the MLR model had 1.6880 RMSE and 27.3787% MAPE. These findings highlight the efficiency of the MLP 4-40-1 model in estimating the exact relationship between the tropospheric parameters and the signal strength of the mobile network in Rivers State. The study provides valuable insights into optimizing network design and emphasizes the significance of including tropospheric parameters in enhancing mobile communication performance.

**Keywords:** Artificial neural network (ANN), Meteorological parameters, Mobile communication, Multiple Linear Regression, Received signal strength (RSS),

BY-NC-ND © *Akinwole and Yussuff* This work is licensed under the **Creative Commons Attribution-Non-Commercial-NoDerivs License 4.0**

# 1.0 Introduction

The troposphere is a dynamic and diverse medium with stratified layers of varying refractive indexes across its expanses. The complexity of this atmospheric region emerges from intricate interactions with prevailing tropospheric parameters and hydrometers, including temperature, relative humidity, atmospheric pressure, and water concentration. As the radio waves propagate through the troposphere, they encounter variations in the refractive index due to changes in tropospheric conditions, making them susceptible to substantial degradation. These changes prompt the radio waves to deviate from their intended straight-line trajectory, giving rise to adverse phenomena like scattering, sub-refraction, super-refraction, and ducting. Each of these effects significantly impairs the quality of the radio link (Grabner et al., 2003; Caglar et al., 2006; Emmanuel et al., 2019). Under unfavorable tropospheric conditions, these effects can lead to heightened signal deterioration and disruption in the radio link. This might influence signal strength, potentially resulting in complete service interruptions and rendering the communication system inaccessible.

Understanding the effects of tropospheric parameters on signal propagation is of crucial importance for the telecommunications industry (Sabri et al., 2018; Julia et al., 2021). With this knowledge, engineers and researchers can design and implement robust communications systems that can adapt to changing weather conditions and ensure consistent performance. Continuous research and efforts to address tropospheric effects can lead to improved signal quality, fewer disruptions, and better services for users, ensuring reliable communication in diverse environmental scenarios.

Numerous research studies have been conducted to evaluate the impacts of tropospheric conditions on RSS across various climate zones and regions (Felix et al., 2017; Kingsley et al., 2018; Mat et al., 2018; Igwe et al., 2021). However, many of these studies have traditionally relied on linear regression or deterministic methods (Adewumi et al., 2013; Famoriji et al., 2013; Ndanusa et al., 2021), which prove inefficient in capturing the intricacies of RSS variability caused by the complexity of the troposphere and fluctuations in meteorological parameters. In recent years, there has been a growing interest in non-mechanistic models for predictive modeling research. Techniques such as exponential smoothing (Ivan et al., 2022), auto regression (Murat, 2021), moving average (Hansun, 2013), multiple linear regression (Gulden, 2013; Seyed et al., 2019), and auto-regressive integrated moving average (Soheila et al., 2016; Bhardwaj et al., 2020; Aweda et al., 2022) have been employed for predicting dependent variables in time series data. The distinguishing characteristic of these approaches is that they develop prediction models based on specific algorithms that focus solely on variations in dependent input data without accounting for the underlying relationships between independent variables and the changing mechanisms.

However, a more sophisticated and widely adopted alternative for time series prediction is the multilayer perceptron neural network (MLP NN). This architecture stands out due to its superior accuracy and precision. The MLP NN performs exceptionally well in predicting inherent complex and non-uniform correlations within a system, even when the underlying mechanisms are not fully understood or lack precision (Litta et al., 2013). Its multi-layered structure allows it to capture intricate patterns and non-linear relationships in data, making it effective in cases where other methods struggle due to data complexity or limited knowledge about the system. This adaptability enables accurate predictions despite uncertainties in underlying mechanisms. The successful implementation of the MLP NN relies on carefully curated experimental datasets, optimized network parameters, and suitable training algorithms (Masoud et al., 2016). Its capability to effectively model and forecast intricate relationships in time series data has made it a popular choice for various applications in research and industry. By leveraging the power of MLP NN, researchers and practitioners can obtain more accurate and reliable predictions of RSS in dynamic and challenging environments affected by tropospheric conditions.

The study aims to examine the effects of tropospheric parameters on RSS in mobile communication networks within Rivers State. Two computational techniques, MLP NN and Statistical MLR are studied to predict the effects of tropospheric parameters on RSS using correlation coefficient, RMSE and MAPE metrics.

### 1.1 *Brief Overview of Multiple Linear Regression Model*

A linear regression technique is utilized to predict future outcomes by employing a best-fit straight line. It can be simple linear regression if only one independent variable is predicted, or multiple linear regression (MLR) when several independent variables are involved. To anticipate how meteorological parameters would affect the RSS, a statistical MLR model is developed. A linear relationship is established between the independent input variables of air temperature, atmospheric pressure, relative humidity, wind speed and the RSS (dependent output variable). The RSS is analyzed and correlated with each independent variable. A general formula for multiple linear regression (MLR) models includes multiple independent variables that are expressed in terms of dependent variables as follows (Orogun, 2021; Ssenyunzi et al., 2021):

$$Y = m + p_1(x_1) + p_2(x_2) + \ldots + p_n + \varepsilon \quad (1)$$

where, $x_1$, $x_2$, $x_3$ are independent variables, Y is the dependent variable which represents the RSS in (dBm); ε = residual error and $p_1$, $p_2$, $p_3$ are regression coefficient, m is the intercept.

### 1.2 *Multi-Layered Perceptron Neural Network (MLP NN)*

Artificial neural networks (ANN) are software simulations that replicate the functionality of the human brain to learn patterns from datasets and then use those patterns to model algorithms for problem solving (Reddy et al., 2022). The ANNs are made up of interconnected processing units called neurons that communicate with one another via a sophisticated branching structure. They acquire information during a learning process from other neurons or the external world in order to improve their performance without the need for human involvement. The data value of the connections between the neurons is stored in the form of bias and weights (Dastres et al., 2021; Balakrishnan et al., 2019). However, the network's weighted connection is modified using a learning rule such as Delta, Hebbian, Perceptron, Outstar, or a correlation learning rule until an optimal result is obtained. The ability of the ANN to learn and independently adjust the error difference between desired output and actual output of the network makes the ANN an effective tool for modeling complex and non-linear relationships as well as predicting underlying patterns in unseen data (Parveen et al., 2016). The accuracy of the ANN and its ability to handle complex tasks depend on a number of variables, such as the learning algorithms for deciding initial weight and order of updating weight, the number of neurons in the hidden layers, and the type of activation functions. Within the neural network, activation functions are applied to match the input pattern to the actual output of the network (Igwe et al., 2021). They offer non-linearity qualities, thus allowing the network to learn complicated features and deliver desired outputs. In the absence of an activation function, regardless of how deep and complex the artificial neural network architecture is, the network effectively operates like a single-layer perceptron. The most frequently utilized activation functions in ANNs are logistic (sigmoid), hyperbolic tangent (Tanh), and rectified linear unit (ReLU) functions.

The multi-layer perceptron (MLP) network is a feed-forward/feed-backward network with one or more intermediate hidden layers connected between the input and the output layers (Shumaila et al., 2018; Igwe et al., 2021). The inner layer communicates with the outside world and sends the information (input data) received as weighted inputs through the hidden layers until it gets to the output layers. Each neuron in the hidden and output layers undergoes a series of transformations using some activation functions so that the output can be easily mapped to the weighted input. The movement of the data from the input layer into the hidden layer and finally to the output layer in one direction is known as feed-forward propagation. To obtain an optimal solution, the weights and bias inputs are continuously adjusted in accordance with some learning rules to reduce the

discrepancy between the actual network output and the predicted output. This training method is known as backward propagation. This entails reversing from the output layer to the hidden layers while adjusting the weight of each neuron in accordance with the loss function from the previous iteration. The MLP model is trained using a supervised learning strategy called Back Propagation.

The output of each node of the hidden layer as shown in Figure 1 is written as,

$$S_{nm} = [\sum_{n=1}^{m}(x_1 * w_{11} + x_2 * w_{21} + \cdots . + x_n * w_{1m}) + b_m \ ] \quad (2)$$

where, $x_1$, $x_2$ and $x_n$ are the inputs of the MLP and the corresponding weights of the input-hidden layer are $w_{1m}$, $w_{2m}$, $w_{nm}$. The weighted sum, $S_{nm}$ with the bias, bm is passed on to the hidden layer via the activation function, f' and is represented as,

$$S_m = f' \ (\sum_{i=1}^{m} x_n * w_{nm} + b_m) \quad (3)$$

Similarly, the output at the output layer of the MLP network is written as,

$$y = f'' \ (\sum_{i=1}^{m} S_m * U_{mi} + c) \quad (4)$$

where, f'' is the activation function used in output layer, the weights, Umi connects the neurons in the hidden layer to the neurons in the output layer, bo is the bias in the output layer. For this study, the proposed MLP NN model is developed using hyperbolic tangent (tanh) and sigmoid (purelin) functions in the hidden and output layers, respectively.

### 1.3 *Performance Evaluation Metrics*

The performance metrics employed to validate the accuracy of the prediction models in this study encompass the Root Mean Square Error (RMSE), Mean Absolute Percentage Error (MAPE) and Pearson correlation coefficient. The RMSE quantifies the average magnitude of the differences between predicted values and actual values. It shows how much the predictions deviate from the true values. The formula for RMSE is as follows:

$$\text{RMSE} = \sqrt{(\sum Predicted - Actual)\text{^}2/N} \quad (5)$$

The MAPE calculates the average percentage difference between the predicted and measured actual value. The formula for MAPE is:

$$\text{MAPE} = (\text{Actual-PredictedActual})N \ * 100 \quad (6)$$

The Pearson correlation coefficient is a measure used to assess the strength of the linear relationship between the tropospheric parameters and signal strength, with values ranging from -1 to 1.

## 2.0 Methodology

The various methods and tools used for data collection and processing are discussed in this section. It includes the development and validation of the statistical and ANN models.

### 2.1 *Data Collection for the Training*

The study was carried out in Borokiri, a suburb of Port Harcourt in Rivers State, which is located within latitude and longitude. A year's worth of meteorological data on the air temperature, atmospheric pressure, relative humidity, and speed was collected from the RSUT NECOP weather station at every five-minute interval. The weather station consists of electronic sensors, a CR 1000 data acquisition system, a wireless measurement system, a power system unit, a wireless telemetry system, solar power, and control systems. It contains a wireless console for communicating and displaying real-time measurements taken at five-minute intervals. The CR 1000 data acquisition system is connected to every component of the weather station through sensors that are very sensitive to instant environmental fluctuations.

The downlink signal strength of a live Globacom Base Transceiver Station (Site: PAR028, Cell ID 35281) in Borokiri was measured using Huawei Mate 10 Pro. This advanced test setup utilized radio frequency signal tracking software within the phone, operating at a frequency of 2600MHz. The measurements were taken every thirty minutes for a period of one year, from January to December 2018. The data were collected on a daily average to determine the correlation between the signal strength of the Global Communication network and the weather parameters. The size of the data is directly influenced by the four meteorological parameters considered. The training dataset comprises 365 data points for these parameters, playing a crucial role in achieving accurate and comprehensive predictions.

### 2.2 *Statistical tool using Multiple Linear Regression (MLR)*

The Multiple Linear Regression is modeled using Microsoft Excel 2018 as,

$$y_{RSS} = b_0 + \sum_{d=1}^{n} b_d x_d \quad (7)$$

W here yRSS denotes the measured signal strength measured in dBm, bo the intercept, bd is [ (b1 = air temperature (oC); b2 = atmospheric pressure (mbar); b3 = Relative humidity (%) and b4 =Wind speed (m/sec)] the coefficient of each independent variable xd: air temperature, relative humidity and atmospheric pressure; n = total number of observation (365).

### 2.3 *Development of MLP NN Model*

The proposed ANN model is built using a supervised learning, three-layered MLP feed forward-back propagation neural network. The three-layered MLP model has one input layer, one hidden layer, and one output layer. The four input variables to the input layer are the measured air temperature (x_temp), relative humidity (x_rh), atmospheric pressure (x_atm. press), and wind speed (x_speed). The hidden layer neurons are varied from 5 to 50 at an interval of 5 to determine the accuracy of the proposed network model. The tanh and purelin activation functions are combined to form a pair of distinct activation functions that are utilized in the hidden and output layers, respectively, with the output layer containing a single neuron for displaying the model's final output. The proposed structure of the three-layered MLP NN is shown in Figure 2.

The input neurons are set of input x*i* for 1≤ *i* ≤3; w_im and u_mk are respectively known as adjustable connection and synaptic weight vectors and where, w_i,m links ith neuron in the input layer to mth neuron at the hidden layer, while u_m,k connects mth neuron at the hidden layer to the kth neuron at the output layer. Each network layer contains the weights, multiplier, summer, bias and activation functions.

### 2.4 *Training and Validation of the Proposed Model*

The proposed MLP NN is designed using the Neural Network Toolbox of MATLAB software. The dataset is made up of a training data set and target data, which are applied to the model to compute its actual output. The input and target data are divided into three subsets, with 80% used for training, 10% for validation, and 10% for testing. The input data is scaled prior to the training phase for consistency between intervals of -1 and +1 in order to achieve the best network performance with the fewest errors. Afterward, the output from the network simulation is restored to its original range. The weight and bias values used are chosen at random. The maximum number of iterations for training is set to 1000. The multilayer network is trained using Levenberg-Marquardt learning algorithms. The number of neurons in the hidden layer is systematically varied in increments of five to assess how it impacts the outcome. The proposed two-layered MLP NN is modeled using the difference between the predicted and measured values. The developed models are validated with the measured RSS values using RMSE and MAPE. Table 4 shows the average Monthly signal strength observed from the Globacom BTS at Borokiri, Rivers State, Nigeria in 2018.

## 3.0 Results and Discussion

### 3.1 *Presentation of Measured Signal Strength*

Figure 3 displays the average daily variations in received signal strength over a twelve-month period, from January to December 2018. Notably, the strongest signal is observed in February at -73.22 dBm, while the weakest occurs in July at -102.844 dBm. The RSS gradually increases at a monthly average of -87.63 dBm from January to February, when it reaches its maximum value at -73.22 dBm (Table 2), and then declines slowly from March through June to July at a minimum value of -102.844 dBm. A slight surge is observed in August,

This journal is © The Nigerian Young Academy 2023

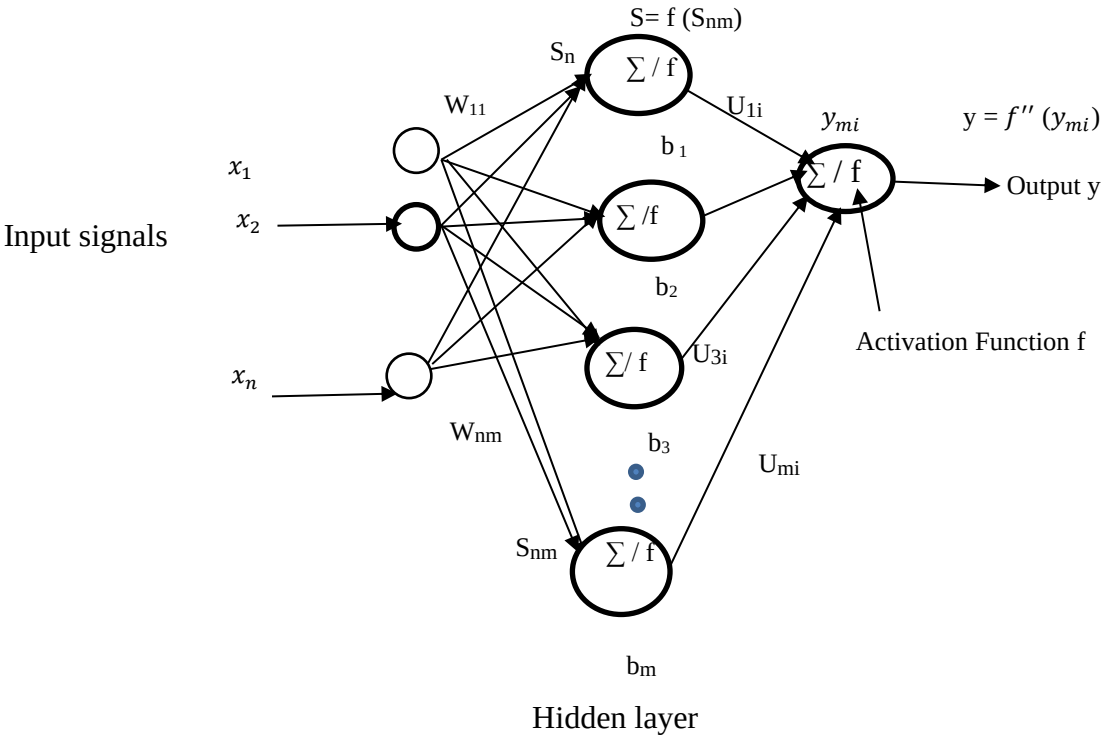



**Figure 1**: Architecture of a multi-layered perceptron (MLP) network

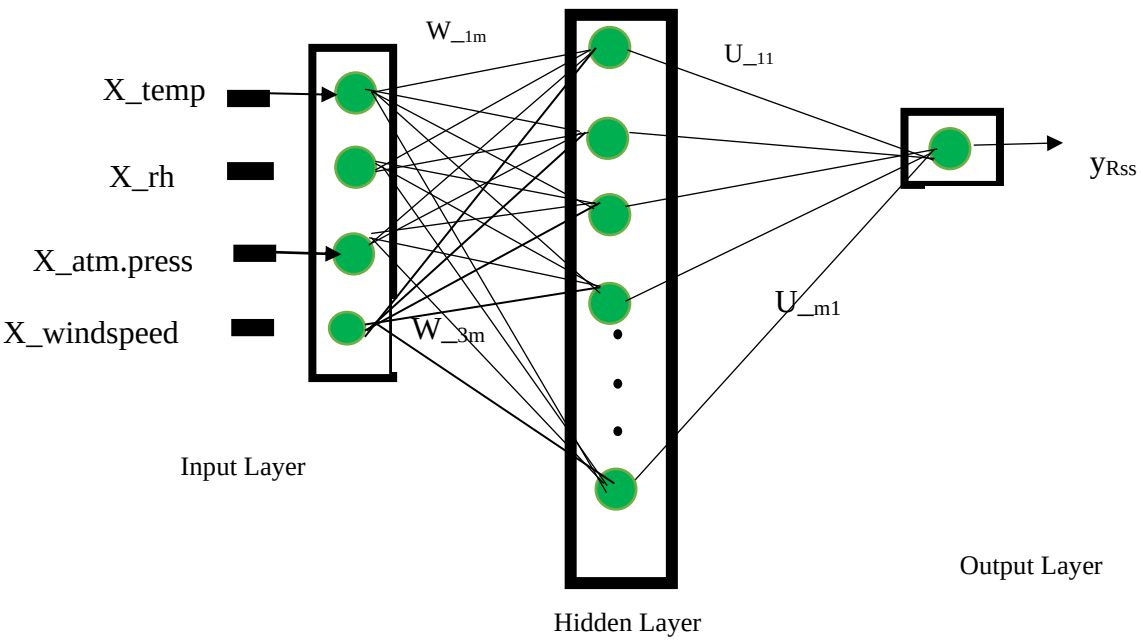



**Figure 2**: Development of Proposed Model

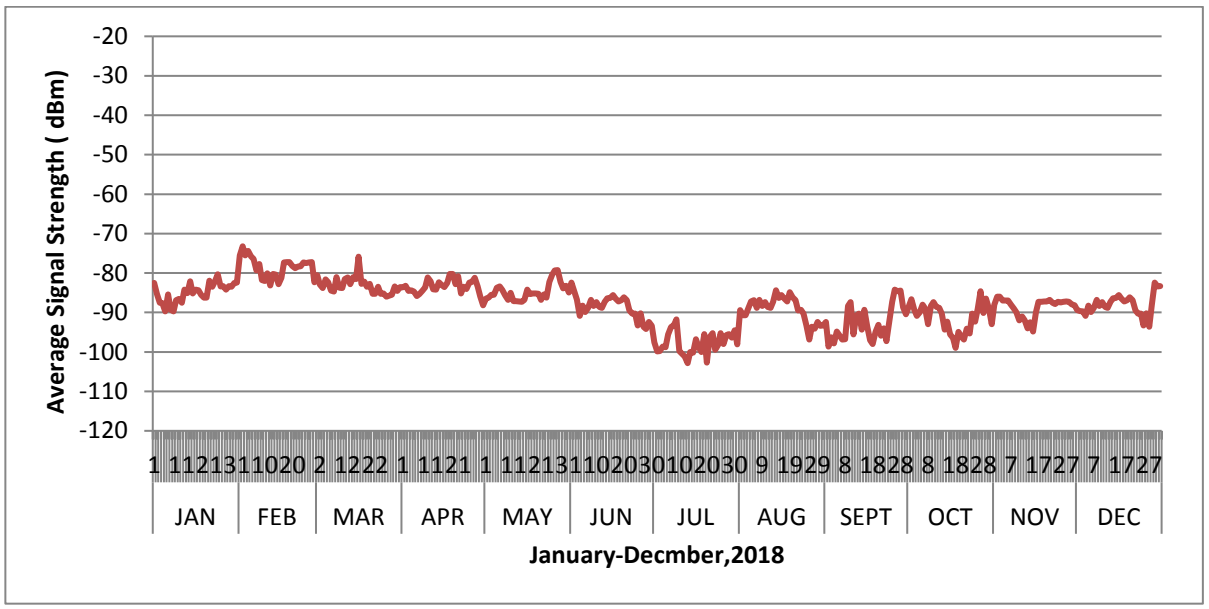



**Figure 3:** Variations in measured RSS from January-December, 2018

**Table 1:** The Average Monthly RSS observed at the Globacom BTS and Average Monthly Meteorological Parameters of Air Temperature, Relative Humidity and Atmospheric Pressure of Borokiri, Port- Harcourt, Rivers State between January-December, 2018

| Months | Received Signal Strength (dBm) | Air Temperature (°C) | Atmospheric Pressure (mbar) | Relative Humidity (%) | Wind Speed (m/sec) |
|---|---|---|---|---|---|
| January | -84.89 | 27.25 | 815.77 | 55.29 | 0.76 |
| February | -78.44 | 29.28 | 814.72 | 63.64 | 0.91 |
| March | -83.13 | 27.91 | 816.83 | 71.26 | 0.96 |
| April | -83.43 | 26.83 | 817.14 | 72.91 | 1.20 |
| May | -84.76 | 26.99 | 816.42 | 67.50 | 1.01 |
| June | -88.59 | 26.56 | 817.65 | 94.71 | 0.97 |
| July | -97.73 | 24.66 | 817.69 | 94.59 | 1.16 |
| August | -89.15 | 24.60 | 817.12 | 81.97 | 0.33 |
| September | -92.71 | 25.24 | 817.46 | 78.77 | 1.14 |
| October | 91.25 | 25.91 | 816.47 | 78.25 | 1.15 |
| November | -88.60 | 26.42 | 815.38 | 97.45 | 0.89 |
| December | -88.07 | 27.38 | 817.20 | 69.01 | 0.88 |

**Table 2** : The Descriptive Statistics for the MLR Model

| | Received Signal Strength (dBm) | Air Temperature (°C) | Atmospheric Pressure (mbar) | Relative Humidity (%) | Wind Speed (m/sec) |
|---|---|---|---|---|---|
| Mean | -87.63 | 26.57 | 816.64 | 75.56 | 0.94 |
| Standard Deviation | 5.55 | 1.77 | 1.99 | 157.53 | 0.35 |
| Median | -87.00 | 24.91 | 816.62 | 75.57 | 0.94 |
| Standard Error | 0.29 | 0.09 | 0.01 | 0.66 | 0.02 |
| Minimum | -102.84 | 22.31 | 806.39 | 40.13 | 0.33 |
| Maximum | -73.22 | 31.93 | 822.07 | 99.30 | 1.86 |

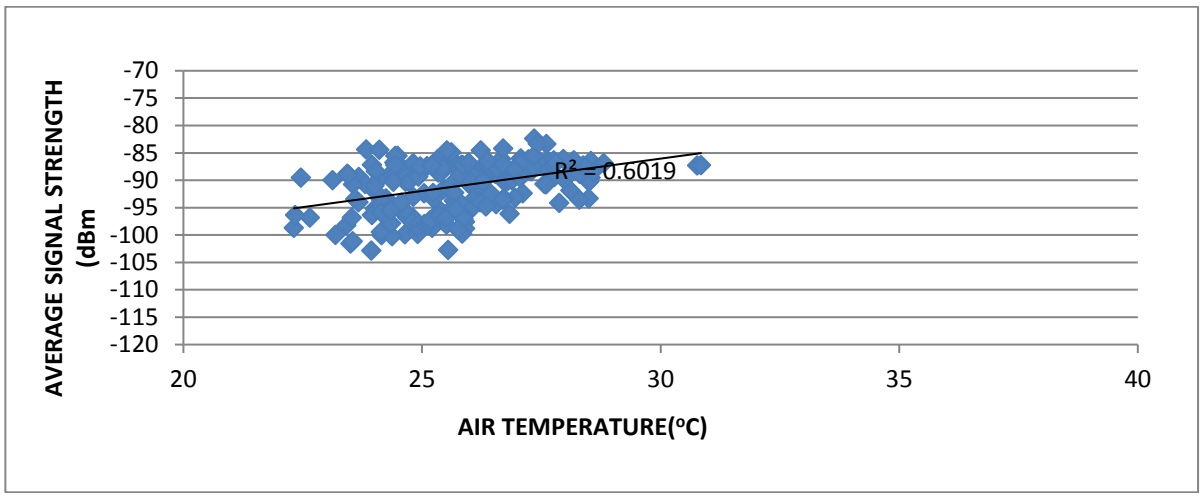



**Figure 4**: A Graph of the Average Measured RSS and the Air Temperature

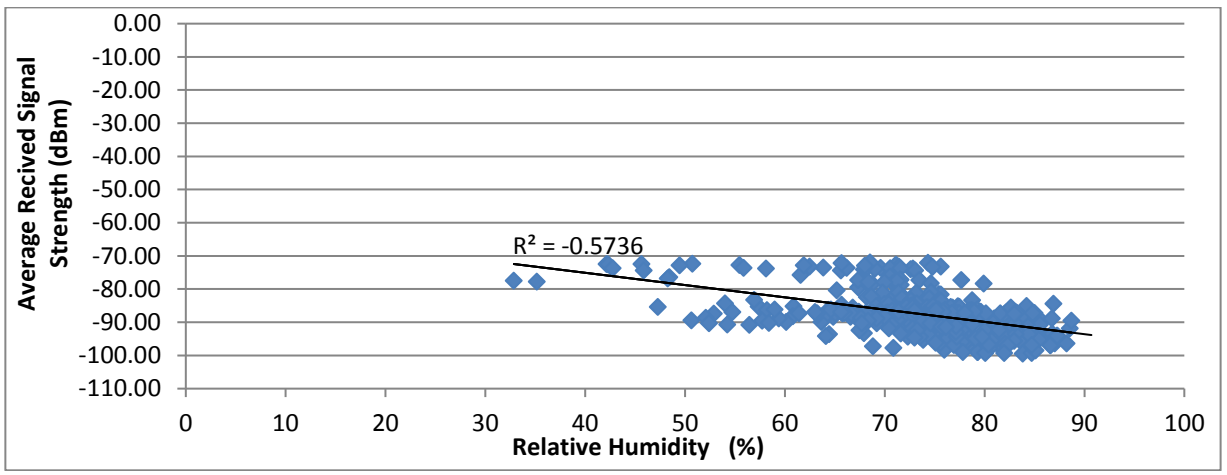



**Figure 5:** A Graph of the Average Measured Signal Strength against the Relative Humidity

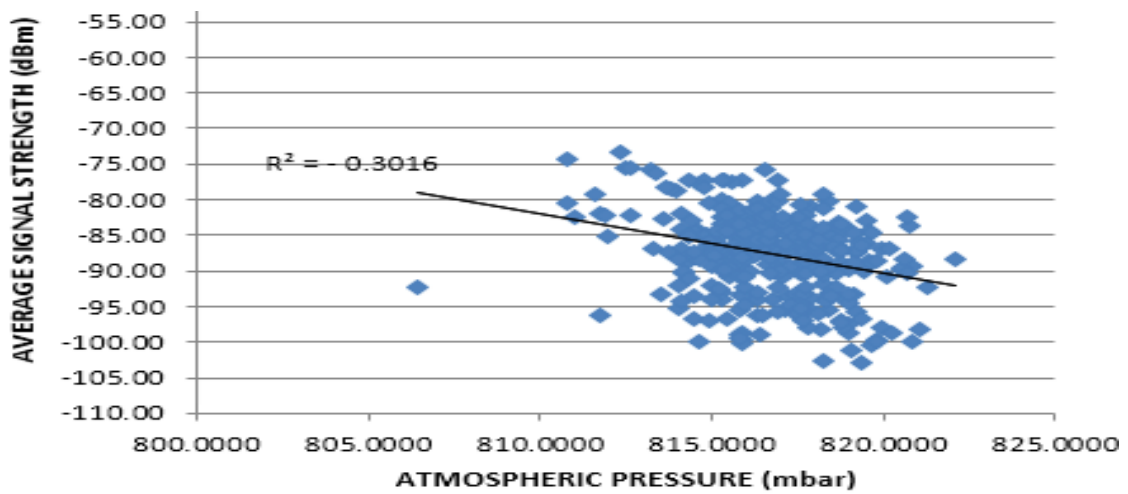



**Figure 6:** A Graph of Signal Strength against Atmospheric Pressure

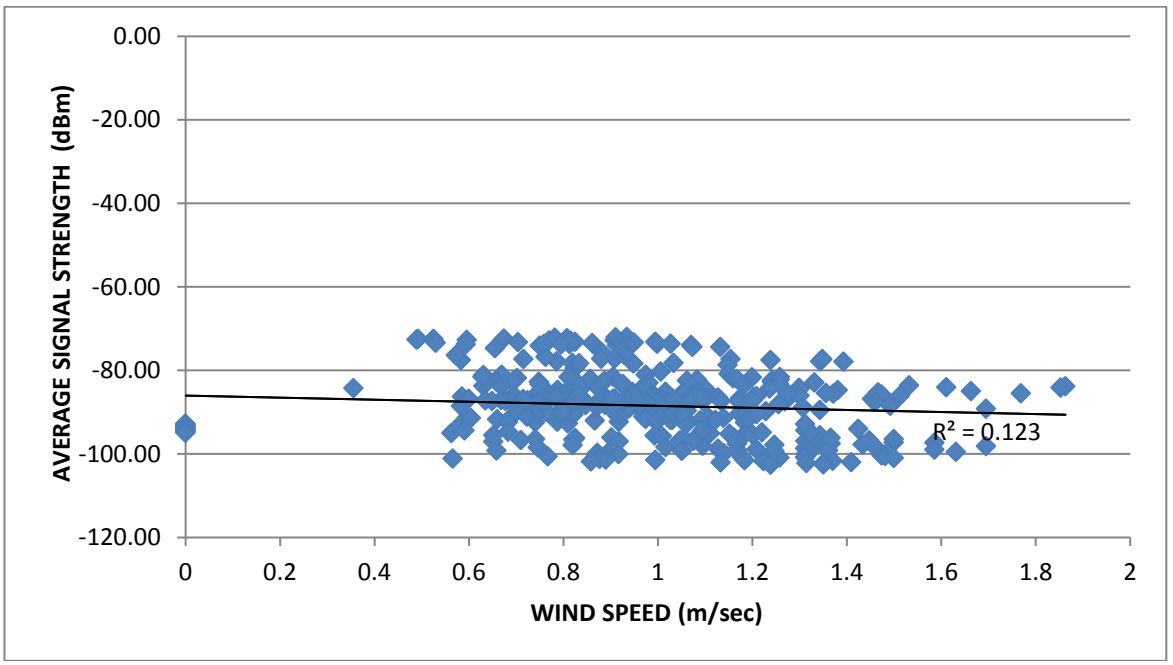



**Figure 7:** A Graph of Signal Strength against Wind Speed

**Table 3**: MLR model summary

| | | | | | | |
|---|---|---|---|---|---|---|
| **Multiple R** | 0.7031 | | | | | |
| **R Square** | 0.4943 | | | | | |
| **Adjusted R²** | 0.4887 | | | | | |
| **Standard Error of the estimation** | 5.5683 | | | | | |
| **No. of observation** | 365 | | | | | |
| **ANOVA: ANALYSIS OF MULTIPLE REGRESSIONCOEFFICIENTS FOR THE MLR MODEL** | | | | | | |
| | **DF** | **SS** | **MS** | **F** | **Sig** | |
| **Regression** | 3 | 10913.22 | 2728.304 | 87.9919 | 0.00 | |
| | | | | **P value** | | |
| **Constant** | 642.5671 | 90.54 | | | | |
| **Air Temperature (°C)** | 3.8898 | 0.14 | 9.2E-18 | 1.55E-21 | | |
| **Relative Humidity** | -1.0031 | 0.11 | 8.3E-05 | 2.35E-7 | | |
| **Atmospheric pressure (mbar)** | -0.2153 | 0.02 | 1.1E-10 | 0.06 | | |
| **Wind Speed (m/sec)** | -0.5172 | | | 0.00 | | |

**Table 4**: The parameters and correlation of the models for the training, validation and testing processes

| Hidden Neurons | Processing time (sec) | Epochs | Training | Validation | Testing |
|---|---|---|---|---|---|
| 5 | 0.14 | 12 | 0.7530 | 0.7851 | 0.7897 |
| 10 | 0.24 | 20 | 0.8513 | 0.6751 | 0.5399 |
| 15 | 0.14 | 12 | 0.8469 | 0.852 | 0.7732 |
| 20 | 0.27 | 22 | 0.9046 | 0.8852 | 0.6571 |
| 25 | 0.19 | 16 | 0.8856 | 0.7659 | 0.7658 |
| 30 | 0.13 | 11 | 0.8754 | 0.8176 | 0.7612 |
| 35 | 0.01 | 14 | 0.8799 | 0.8429 | 0.7901 |
| 40 | 0.01 | 10 | 0.8368 | 0.8026 | 0.8473 |
| 45 | 0.01 | 13 | 0.8959 | 0.6712 | 0.8187 |
| 50 | 0.01 | 11 | 0.8383 | 0.5960 | 0.7452 |

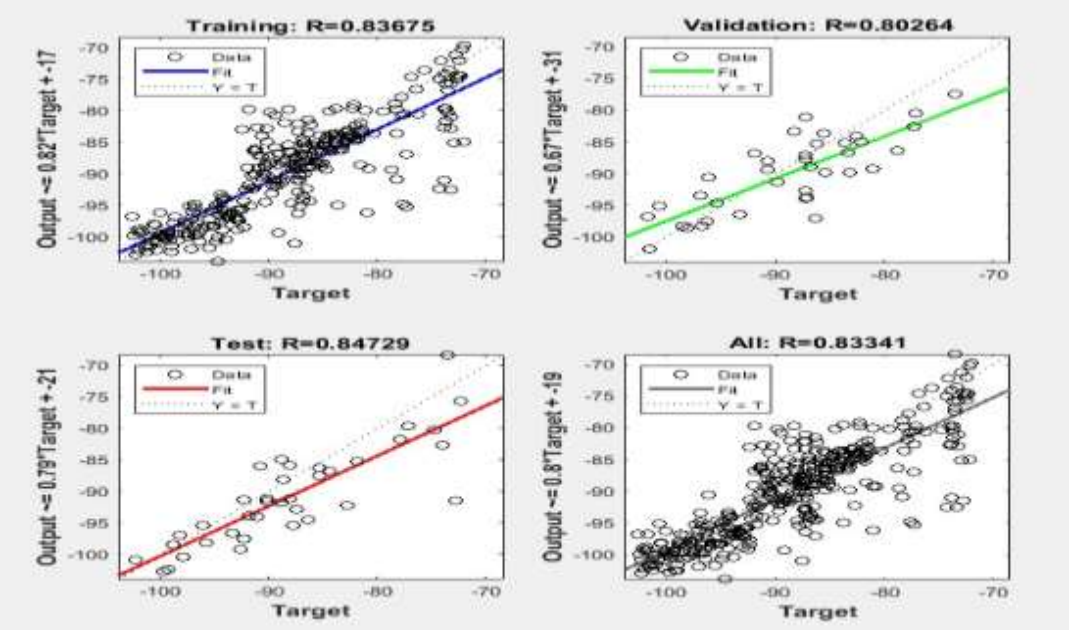



**Figure 8**: MLP Model with Hidden Layer of 40 Neurons

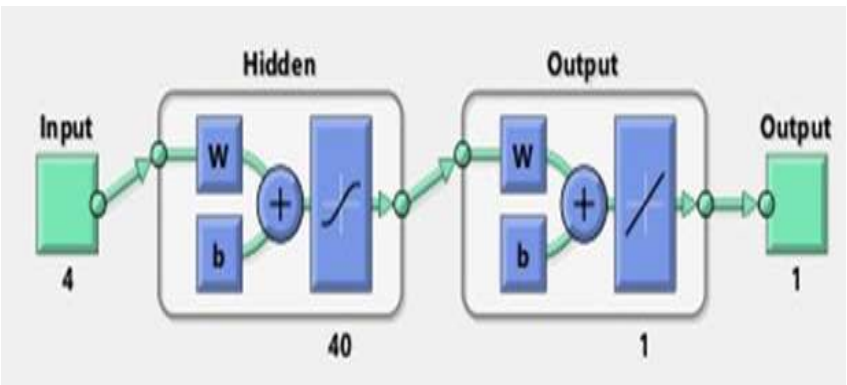



**Figure 9:** The Structure of the Proposed 4-40-1MLP NN Model

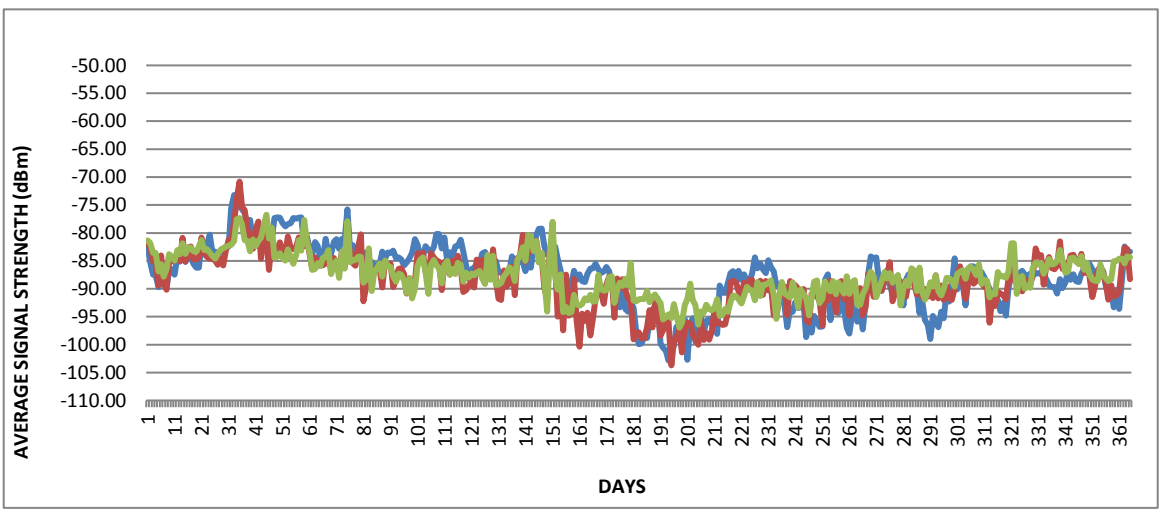



**Figure 10**: Measured RSS with Predicted RSS

peaking at -84.15 dBm. In September and October, a marginal decline is observed, attributed to transient disturbances or signal fluctuations. However, in November, the RSS moderately increased, with a monthly average of -88.60 dBm. It then decreases again in December, reflecting expected seasonal variations and potential adverse weather conditions affecting signal propagation. This provides insights into the dynamic nature of RSS variation over the year, offering essential information for optimizing signal coverage and understanding signal propagation behavior.

According to Table 2, the atmospheric pressure shows an upward trend, rising from 806.39 mbar to 822.07 mbar, with an average value of 816.67mbar. This suggests a possible weather pattern of high-pressure systems dominating the area. The air temperature exhibits a range between 22.31°C to 31.93 °C, with an average value of 26.57 °C, indicating diverse weather conditions. The relative humidity has maximum and minimum values of 40.13% and 99.30%, with an average value of 75.57%. This suggests fluctuations in moisture levels in the atmosphere. Lower humidity values may indicate dry conditions, while higher values could indicate more humid weather. The region experiences varying speeds, ranging from 0.33 to 1.86 m/sec, with an average of 0.94m/sec. From January to April, the region experiences lower humidity and relatively lower temperatures. Throughout this period, wind speeds remain at a moderate level, providing better signal propagation and minimizing signal loss. As a consequence, signal strength remains more consistent during these months. From May to October, higher humidity levels prevail, leading to more prevalent and stronger breezes, driven by gusty winds during thunderstorms and heavy rainfall. However, during this period, there are occasional moments of calmness in August due to lower humidity levels and dry atmospheric conditions. These calm intervals result in improved RSS. In December, the region experiences cooler temperatures with less atmospheric turbulence, leading to calmer wind speeds. The reduction in wind speed during this time contributes to further improvements in RSS and communication reliability.

Figure 4 depicts a graph of the average RSS in relation to air temperature. There is a positive correlation ($R^2$= 0.6109) between the two, indicating that a slight increase in air temperature results in a significant rise in RSS and vice versa. This correlation is influenced by humidity changes resulting from temperature variations, affecting overall RSS. In January and February, RSS notably increases as the air temperature rises from an average of 27.25 2°C to 29.28°C From March to July, the RSS gradually decreases with a slight reduction in air temperature, but in July, there is a considerable drop in air temperature, causing strong fluctuations and a reduction in RSS. In August, there is a slight fluctuation in RSS due to a minor temperature variation from the previous month, July. Strong RSS fluctuations occur from September to October, despite slight variations in air temperature. The air temperature variations decrease toward December, indicating slight fluctuations in RSS.

The RSS is also affected by the amount of moisture in the form of water vapor in the atmosphere. The correlation between the measured RSS and the relative humidity, as shown in Figure 5, indicates a negative moderate correlation (-0.5736) and an inverse relationship between the measured RSS and relative humidity when other meteorological parameters are constant. As the level of water content in the air decreases, the measured RSS tends to increase. From January to March, variations in humidity cause minor fluctuations in the RSS. In April, the variations in relative humidity showed no significant effects on the RSS. However, from May to July, an increase in relative humidity results in strong fluctuations in the RSS. During August, there is a sharp decrease in relative humidity due to the 'August break', leading to a rise in RSS caused by lower moisture levels in the air. From September to October, the RSS experiences fluctuations due to sharp variations in relative humidity. This trend continues until November, when a slight decrease in relative humidity causes an increase in RSS. In December, fluctuations in relative humidity led to a slight variation in the RSS.

The observed patterns highlight how changes in relative humidity can impact the RSS and, consequently, the performance of the communication system throughout the year. Decreased relative humidity can lead to signal attenuation. When the air is drier, it has a lower ability to support the propagation of electromagnetic waves, resulting in weaker signal strength at the receiving end. This can lead to data loss, interference, and reduced signal range and coverage.

The relationship between variations in atmospheric pressure and the RSS exhibits a weak negative correlation of -0.3016, as illustrated in Figure 6. The measured RSS shows an inverse proportionality with changes in atmospheric pressure. During the months of January to March, the variations in atmospheric pressure have minimal significant effects on the RSS. However, from April to July, there is a slight rise and reduction in atmospheric pressure as radio waves travel through the troposphere, leading to scattering and absorption of signals. This phenomenon results in strong fluctuations in the RSS. In August, the atmospheric pressure experiences a decline due to the 'August break', resulting in less RSS fluctuation. However, fluctuations in atmospheric pressure continue thereafter, corresponding with a decrease and increase in RSS.

The relationship between received signal strength and wind speed is not one of complete independence. This connection is evidence by a noticeable positive correction as depicted in Figure 7. However, it is important to highlight that wind speed does not directly influence the received signal strength of mobile communication networks. The relatively weak positive correlation of 0.123 underscores a minimal connection between signal strength and wind speed. Nevertheless, it is crucial to acknowledge that the effect of wind speed extends beyond its impact on RSS, potentially influencing the physical environment and, by extension, the stability of communication infrastructure. Specifically, strong winds could result in misalignment of antennas on towers or satellite dishes, leading to adverse effects such as decreased signal strength or increased interference. It is crucial to take into account the influence of this parameter on the system to ensure reliable communication.

### 3.2 *Presentation of Multiple-Linear Regression (MLR) Model*

The MLR model exhibits moderately positive atmospheric pressure and relative humidity. Table 3 displays the corresponding correlated coefficients, the p-values, and the standard error values for each meteorological parameter as determined by the MLR analysis. The p-values ($p \leq 0.05$) indicate that the three independent meteorological parameters are highly significant. The correlation coefficients of the air temperature, relative humidity, atmospheric pressure, and wind speed are estimated as 0.6109, -0.5736, -0.3016, and 0.123, respectively, using 2010 Microsoft Excel software. As shown in Table 3, the air temperature is highly significant and exhibits a moderately positive correlation with the RSS. The atmospheric pressure is characterized as having a negative correlation with the RSS, though weak and statistically significant. The relative humidity exhibits a great influence and a positive moderate correlation on the RSS.

The $R^2$ value of 0.4943 in Table 3, reveals a linear relationship between the dependent and independent variables. This means that the predictor variables (temperature, relative humidity, atmospheric pressure, and wind speed) collectively have a significant influence on explaining the variance in the dependent variable (received signal strength). The equation for the MLR model is given as follows:

$$Y_{RSS} = 642.5671 + 3.8898^{*} x_{temp} - 1.0031^{*} x_{rh} - 0.2153^{*} x_{atm.pres} - 0.5172^{*} x_{ws} \quad (9)$$

Although a weak correlation is indicated by this value, the MLR model is highly significant and can specifically describe the influence of air temperature, atmospheric pressure, and relative humidity on the RSS. The weak prediction of the MLR model as given by the $R^2$ is an indication of its linearity ability, which is considered a limitation when handling non-linear relationships. They are considered ineffective when complex and non-linear relationships are involved.

### 3.3 *Presentation of MLP Neural Network Model*

Prior to the design of the MLP neural network, datasets were read using the import tool. The network models are trained using the Levenberg Marquardt algorithm and simulated in the hidden and output layers, respectively, using hyperbolic tangent (tanh) and linear activation (purelin). The effects of the number of hidden layer neurons on the performance of the network are verified by training the MLP network with different numbers of neurons, ranging from 5 to 50. The

performance of the regression model is evaluated, and the results, including the regression plot for each model, are presented in Table 4.

### 3.4 *Regression Analysis*

The performance of the ten MLP NN models developed is evaluated and verified using the correlation coefficient, $R^2$. The regression plots show the accuracy of the model predictions compared to the actual target values (measured RSS). The solid line (red color) depicts the best linear fit, while the dash line indicates the perfect line. The $R^2$ of each trained network is presented in Table 3. The results show that MLP with 40 neurons after 10 iterations exhibits the best fit with correlation coefficients of 0.8368, 0.8026, and 0.8473 for the training, validation, and testing processes, respectively, as shown in Figure 8. The performance evaluation of the 4-40-1 MLP NN indicates a strong correlation between the meteorological parameters and the measured RSS.

The correlation between tropospheric parameters and measured RSS is notably stronger at 0.7942, unlike the MLR model with a correlation coefficient of 0.2164 using Pearson correlation coefficient. The MLP NN outperforms the MLR model with a higher $R^2$, providing better predictions of the non-linearity in the datasets.

The architecture of the proposed network model, 4-40-1 is shown in Figure 9. The predicted RSS values of the model were validated with the observed RSS data obtained from field measurement and the results are shown in Figure 10.

It is evident that the MLP NN demonstrates superior predictive accuracy, closely aligning with the measured values and surpassing the performance of the MLR model. The MLP achieves an RMSE of 0.2480 and a remarkably low MAPE of 12.9963%, while the MLR model yields an RMSE of 1.6880 and a MAPE of 27.3787%.

## 5.0 Conclusions

The complexity of the atmosphere is influenced by variations in atmospheric conditions during radio wave propagation, which significantly affect the RSS of radio waves. This study is focused on examining the effects of tropospheric parameters, including air temperature, relative humidity, atmospheric pressure, and wind speed, on received signal strength. The findings indicate a moderately positive correlation of 0.6109 between air temperatures and signal strength, as deduced from the analysis of measured atmospheric parameters. To put it differently, an increase in air temperature tends to coincide with an increase in RSS. This implies that higher temperatures could lead to stronger signals. Conversely, relative humidity tends to weaken received signals. The correlation between the signal strength and relative humidity is found to be -0.5736. This effect stems from the presence of water vapor in the atmosphere, which acts as a partial reflector for radio waves. Similarly, atmospheric pressure shows a weak negative correlation of -0.3016, suggesting a slight decrease in signal strength with higher atmospheric pressure is experienced between atmospheric pressure and RSS. The weak positive correlation of 0.123 between the wind speed and received signal strength indicates a minor association between them.

The computational tools are employed to assess the intricate relationship between tropospheric parameters and signal strength. Notably, the MLP NN model demonstrates superior performance compared to the MLR, yielding accuracy with a 1.6880 RMSE and a 27.3787% MAPE, in contrast to the RMSE of 0.2480 and MAPE of 12.9963% from the MLR. The MLR model displays a correlation coefficient of 0.2164, signifying a weaker correlation, while the MLP model showcases a more robust correlation coefficient of 0.7942. The results show the proficiency of the MLP NN in capturing inherent non-linear relationship between the tropospheric parameters and RSS, which might be less apparent when using MLR method. However, it is crucial to consider the effects of meteorological parameters when designing and maintaining communication networks to ensure their stability and reliability, especially in areas prone to severe weather conditions. Therefore, network planners require accurate knowledge of meteorological parameters and their impact on radio signals to design reliable and efficient radio communication systems. To enhance the study's relevance and depth, it is recommended that a broader array of tropospheric parameters over an extended period for unique atmospheric traits should be considered.

## Declaration of Conflict of Interests

All authors have declared that there are no conflicts of interest

## Authors' Contributions

Conception: ABH,AIOY
Design: ABH
Execution: ABH
Interpretation: ABH
Writing the paper: ABH,AIOY

## Reference

Adewumi, A.S., Alade, M.O., and Adewumi, H.K. (2013). Influence of Air Temperature, Relative Humidity and Atmospheric Moisture on UHF Radio Propagation in South Western Nigeria. International Journal of Science and Research (IJSR), 4(8): 588-592. https://api.semanticscholar.org/CorpusID:28223009

Aremu, O.A., Oyinkanola, L.O., Akande, A., and Azeez, W.A. (2018). Effects of Radio Refractivity Gradient and K-Factor on Radio Signal over Ibadan, South Western, Nigeria. Global Scientific Journals, 6(5): 248-252. https://www.globalscientificjournal.com/research/effects_of_refractivity_gradient_and_k_factor_on_radio_signal_over_ibadan_western-nigeria

Aweda, F.O., Olufemi, S.J., and Agbolade, J. O. (2022). Meteorological Parameters Study and Temperature Forecasting in Selected Stations in Sub-Sahara Africa using MERRRA-2 Data. Nigerian Journal of Technological Development, 19(1): 80-91. https://www.researchgate.net/publication/360335259_meteorological_parameters_study_and_temperature_forecasting_in_selected_stations_in_sub-sahara_africa_using_merra-2_data

Balakrishnan, H. N., Aditi, K., Snehanshu, S., and Nithin, N. (2019). ChaosNet: A Chaos based Artificial Neural Network Architecture for Classification: Review of Chaos. An Interdisciplinary Journal of Nonlinear Science, 29(11): 1-18. https://doi.org/10.1063/1.5120831

Bhardwaj, R., and Duhoon, V. (2020). Auto-Regressive Integrated Moving-Averages Model for Daily Rainfall Forecasting. International Journal of Scientific & Technology Research, 9(2): 793-797. https://www.researchgate.net/publication/340476187_auto_regression_integrated_moving_averages_model_for_daily_rainfall_forecasting

Caglar, Y., Peter G., and William, S.H. (2006). Estimation of Radio Refractivity from Radar Clutter using Bayesian Monte Carlo Analysis. IEEE Transactions on Antennas and Propagation, 54(4): 1318-1327. https://ieeexplore.ieee.org/document/1614189

Dastres, R., and Soori, M. (2021). Artificial Neural Network Systems. International Journal of Imaging and Robotics , 21(2): 13-25. https://hal.science/hal-03349542/document

Eichie, J.O., Agidi, E.O., and Oyedum, O.D. (2021). Atmospheric Temperature Prediction across Nigeria using Artificial Neural Network. 5th International Conference on Future Networks and Distributed Systems (ICFNDS): 280-286. https:// dl.acm.org/doi/abs/10.1145/3508072.3508114

Emmanuel, I., Adedayo, K.D., Adeyemi, B., and Ojo, O.S. (2019). Meteorological Parameter Anomalous Radio Propagation over Nigeria. Nigeria Journal of Pure & Applied Physics, 9(1): 34-40. https://doi.org/10.4314/njpap.v9i1.7

Famoriji, O.J., and Olayinka, M.O. (2013). A Test of the Relationship between Refractivity and Radio Signal Propagation for Dry Particulates. Research Desk, 2 (4): 334-338. https://www.researchgate.net/publication/345765268_a_test_of_the_relationship_between_refractivity_and_radio_signal_propagation_for_dry_particulates

Felix, A., Olufemi, A.A., Ibrahim, H.D., Ayegba, A., Olu, J.J., and Fonyuy, W.D. (2017). Investigation of the Influence of Atmospheric Temperature and Relative Humidity on FM Radio Signal Strength: A case study of WE FM Abuja. International Journal of Scientific and Technology Research, 6 (11): 70-74. https://www. semanticscholar.org/CorpusID:114886635

Grabner, M., and Kvicera, V. (2003). Refractive Index Measurement at TV Tower Prague. Radio Engineering, 12(1): 5-7. https://www.researchgate.net/publication/26511549_refractive-_index-measurement-at-tv-tower-plague

Guden, K.U., and Nese, G. (2013). A Study on Multiple Linear Regression Analysis. 4th International Conference on New Horizon in Education,106: 234-240. https://www.researchgate.net/publication/260015447_a_study_on_multiple_linear_regression_analysis

Hamza, M.G., Latiff, L.A., Mustafa, E.M., and Gasim, W.M. (2017). Radio Propagation and Troposphere Parameters Effect for Microwave Links in Sudan. IEEE International Conference on Communication, Control, Computing and Electronics Engineering , 3: 1-5. https://ieeexplore.ieee.org/document/7867670

Hansun, S. (2013). A New Approach of Moving Average Method in Time Series Analysis. International Conference on New Media Studies (CoNMedia): 1-4. https://ieeexplore.ieee.org/iel7/6698927/6708534/06708545

Igwe, E., and Ukoette, E. (2021). Influence of Troposphere Variables on Signal Strengths of Mobile Networks in Calabar Nigeria. Journal of Scientific and Engineering Research, 8(9): 137-145. https://www.researchgate.net/publication/355164592_influence_of_tropospheric_variables_on_signal_strengths_of_mobile_networks_in_calabar_nigeria

Igwe, K. C., Oyedum, O.D., Aibinu, A.M., Ajewole, M.O., and Moses, A.S. (2021). Application of Artificial Neural Network Modeling Techniques to Signal Strength Computation. ScienceDirect, 7(3): 1-9. https://www.sciencedirect.com/science/articles/pii/S2405844021001523

Javeed, S., Alimgeer, K.S., Javed, W., Atif, M., and Uddin, M.A. (2018). A Modified Artificial Neural Network based Prediction Technique for Tropospheric Radio Refractivity. Public Library of Science one (PLOS one), 13(3): 1-17. https://pubmed.ncbi.nlm.nih.gov/29494609/

Litta, A. J., Sumam, M. I., and Mohanty, U. C. (2013). Artificial Neural Network Model in Prediction of Meteorological Parameters during Premonsoon Thunderstorms. International Journal of Atmospheric Science , 2013(525383): 1-14. https://doi.org/10.1155/2013/525383

Masoud, A., Afshin, A. N., Mohsen, H., Hooman, Y., and Dahari, M. (2016). Predicting the Viscosity of Multi-Walled Carbon Nanotubes/Water Nanofluid by Developing an Optimal Artificial Neural Network based on Experimental Data. International Communications in Heat and Mass Transfer, 77: 49-53. https://doi.org/10.1016/j.icheatmasstransfer.2016.07.008

Mat, R., Hazmin, S. N., Umar, R., Ahmad, S., Zafar, S. N. A. S., and Marhamah, M.S. (2018). The Modeling of Tropical Weather Effects on Ultra High Frequency (UHF) Radio Signal using Smart PLS. IOP Conference Series: Material Science and Engineering. 440: 1-8. https://doi.org/10.1088/1757-899x/440/1/012041

Mehrmolaei, S., and Keyvanpour, M. R. (2016). Time Series Forecasting using Improved ARIMA. Artificial Intelligence and Robotics (IRANOPEN): 92-97. https://ieeexplore.ieee.org/document/7529496

Mirbagheri, S.A., and Mohammadi, M. (2019). Prediction of Environment Effects in Received Signal Strength in FM/TV Station based on Meteorological Parameters using Artificial Neural Network and Data Mining. Journal of Environmental Management, 250: 1-7. https://doi.org/10.1016/j.jenvman.2019.109454

Murats, A. (2021). Vector Autoregressive Model and Analysis, Handbook of Research on Emerging Theories. Models and Applications of Financial Econometrics: 197-214. https://doi.10.1007/978-3-030-54108-8

Ndanusa, B., Yusuf, S. D., Umar, I., Kwaha, B. J., and Muhammad, B. L. (2021). Evaluating the Effects of Selected Atmospheric Parameters on Signal Reception of Direct Broadcasting Satellite at Ku-Band in North Central, Nigeria. African Scholars Journal of Pure and Applied Science, 22(9): 5-30. http//www.africanscholarpublications.com/wp-content/uploads/2021/S_Vol22_No9_September2021-2. pdf

Parveen, R., Nabi, M., Memon, F.A., Zaman, S., and Ali, M. (2016). A Review and Survey of Artificial Neural Network in Medical Science. Journal of Advance Research in Computing and Applications, 3(1): 7-16. https://www.akademiabaru.com/doc/ARCAV3_N1_P7_16

Reddy, S.M., Babu, P.A., Maharshi, G.CH.S.S., Kumar, B.P., and Shankar, P.B. (2022). A Review on Artificial Neural Networks, International Journal of Research Publication and Reviews, 3(4): 166-169. https://www.researchgate.net/publication/359710146_a_review_on_artificial_neural_networks

Sabri, N.H., Zafar, S. N. A. S., Umar, R., and Mat, R. (2018). Northeast Moonsoon Effect on Ultra High Frequency (UHF) Signal Attenuation at Kusza Observatory. IOP Conference Series: Journal of Physics, 1152 (2019): 2-9. https://www.researchgate.net/publication/331470333_northeast_monsoon_effect_on_ultra_high_frequency_uhf_signal_attenuation_at_kusza_observatory

Ssenyunzi, C. R., Oruru, B., and D'ujanga, M. F. (2021). Linear Regression Models to Predict the Troposheric Parameters at the Global Positioning Systems'sites over the East African Region. East African Journal of Science, Technology and Innovation, 2(3): 1-17. https://doi.org/10.37425/eajsti.v2i3.274

Svetunkov, I., Kourentzes, N., and Ord, J.K. (2016). Complex Exponential Smoothing. Naval Research Logistics, 69(8): 1108-1123. https://www.researchgate.net/publication/283488877_complex_exponential_smoothing

Ukhurebor, K.E., and Azi, S.O. (2019). Review of Methodology to obtain Parameters for Radio Wave Propagation at Low Altitudes from Meteorological Data: New Results for Auchi Area in Edo State, Nigeria. Journal of King Saud University, 31(4): 1445-1451. https://www.researchgate.net/profile/Kingsley_Ukhurebor/publication/323633607_review_of_methodology_to_obtain_parameters-for_radio_wave_propagation_at_low_altitudes_from_meteorological_data_new_results_for_auchi_area_in_edo _state_nigeria



This journal is © The Nigerian Young Academy 2023